Archive of Applied Mechanics (2021) 91:3665–3677
https://doi.org/10.1007/s00419-021-01953-x

ORIGINAL

Fabian Jaeger · Alessandro Franceschi · Holger Hoche · Peter Groche · Matthias Oechsner

Statistical analysis of the reproducibility of residual stress measurements in cold extruded parts

Received: 2 November 2020 / Accepted: 30 March 2021 / Published online: 27 April 2021
© The Author(s) 2021

Abstract Cold extruded components are characterized by residual stresses, which originate from the experienced manufacturing process. For industrial applications, reproducibility and homogeneity of the final components are key aspects for an optimized quality control. Although striving to obtain identical deformation and surface conditions, fluctuation in the manufacturing parameters and contact shear conditions during the forming process may lead to variations of the spatial residual stress distribution in the final product. This could lead to a dependency of the residual stress measurement results on the relative axial and circumferential position on the sample. An attempt to examine this problem is made by the employment of design of experiments (DoE) methods. A statistical analysis of the residual stress results generated through X-Ray diffraction is performed. Additionally, the ability of cold extrusion processes to generate uniform stress states is analyzed on specimens of austenitic stainless steel 1.4404 and possible correlations with the pre-deformed condition are statistically examined. Moreover, the influence of the coating, consisting of oxalate and a MoS_2 based lubricant, on the X-Ray diffraction measurements of the surface is investigated.

Keywords 316 L · 1.4404 · Austenitic stainless steel · Residual stresses · Cold extrusion · X-ray diffraction · $Sin^2\ \Psi$ · Design of experiments

1 Introduction

Residual stresses can influence the component behavior in positive and negative fashions [1]. Compressive residual stresses generally lead to components being more resilient to fatigue, while tensile stresses can cause premature failures [2, 3]. This effect becomes more relevant as the design of engineering components includes reduced safety margins [4]. Therefore, knowledge of the mechanisms between residual stresses and material properties and the feasibility to produce the desired residual stress state components rise in importance. For further research in this direction, it is important that residual stress measurements on the surface are reproducible both at the same position as well as for varied measurement positions. The change of the residual stress state of austenitic steels shaped by cold extrusion at various depths has been researched extensively [5, 6]. From the surface to depths of 1 mm, changes in the residual stress up to 800 MPa have been observed. On the surface, local shearing effects complicate measurements of the residual stresses. Despite these difficulties, the measurement of the residual stress state is of paramount importance for both research and industrial applications. For quality control in production lines, removing material to measure the residual stresses below the surface would damage

F. Jaeger (✉) · H. Hoche · M. Oechsner
Center for Structural Materials MPA-IfW, Technische Universität Darmstadt, Grafenstr. 2, 64283 Darmstadt, Germany
e-mail: fabian.jaeger@tu-darmstadt.de

A. Franceschi · P. Groche
Institute for Production Engineering and Forming Machines, Technische Universität Darmstadt, Otto-Berndt-Straße 2, 64287 Darmstadt, Germany

the produced workpieces and would thus be undesirable. For scientific use, the damage to samples through the measurement in greater depths is a problem, if other properties resulting from the residual stress state are to be investigated afterward. Additionally, the surface state is of the utmost importance for crack initiation and failure under cyclic loads. Therefore, it is imperative to gain reliable information from measurements at the surface. Research about optimizing the measurement parameters for the difficulties caused by coarse-grained microstructures has already been conducted [5]. In this research, it was shown that the worsening of measurement results by coarse grain effects can be alleviated by choosing a longer exposure time, introducing Ψ oscillation and ϕ-rotation, or utilizing a collimator with a bigger diameter. Additionally, a criterion for assessment of the quality of measurements was determined using the R^2-value of the peak fit.

With eventual problems of coarse grain effects researched, the other difficulty of judging how significant a single measured point is for the whole sample are possible changes of the residual stress result when measuring at a different position. For cold extruded samples with cylindrical geometry, the measurement position can vary in two ways: by the length along the sample and the angle along the circumference. Regarding the length along the sample, measurements have been performed on ferritic steels [7]. In those, the scatter spanned up to 200 MPa. Research for rotary swaged samples made of austenitic steel [8] has shown that this process leads to unpredictably varying residual stress states along the circumference (scatter of up to 500 MPa). However, despite the many simulated residual stress distributions [9], there have been no 2D-mappings of the residual stress state on cylindrical cold extruded workpieces made of austenitic steel.

Another difficulty, which could interfere with the significance of residual stress measurements at the surface of cold extruded samples, is the lubricant layer, which is usually used to minimize friction during the cold working process. This coating consists of one layer of oxalate and one of MoS_2, which has a thickness of a few μm.

The aim of this work is to identify the suitability of a single measurement to be significant for the whole sample under the aspect that the sample extends in both longitudinal and lateral direction. Additionally, it will be checked, whether the removal of the lubrication layer is necessary for satisfactory results.

1.1 State of the art

Residual stresses are categorized into three classes: First-order residual stresses are on the macroscopic scale and change along the workpiece, second-order residual stresses describe the stresses between grains of different orientation and have ranges of a few μm, and third-order residual stresses are caused by lattice defects and have ranges on the same scale (a few nm) [10]. In all cases, these three orders of residual stress are superimposed onto each other. X-ray diffraction methods can be utilized to quantify the residual stresses by measuring the shift of the Bragg-reflexes of diffraction, which is caused by the residual stresses influencing the atomic distances in the crystal lattices.

Each component exhibits a residual stress state, which is influenced by its manufacturing process, affects its employment. This is essential due to the processes performed in the manufacturing of the part. Therefore, through an attentive study of the manufacturing chain with regard to the residual stress formation, the performances of a mechanical components can be improved or deteriorated. Residual stresses in forming operations mainly have three causes: inhomogeneous plastic deformations, thermal gradients or phase changes [4]. Depending on the considered process, these three causes have a different contribution to the final stress state. The residual stresses are often due to a combination of these causes, therefore multi-physics models may be needed for a precise prediction.

In both the measurement as well as simulation of residual stresses, it is usually assumed that geometrical symmetries lead to symmetrical residual stress states, i.e., there should be no dependency from the measurement position [11]. Therefore, if results of various different measurement positions are compared, one would expect different residual stress states due to different degrees of deformation[12]. Research showed the assumption of a homogenous stress state was not valid for rotary swaging[8]. In this research, samples were measured at relative angles of 0°, 18°, 36°, 54°, 72°, 90°, 180° and 270° with resulting differences of the residual stresses as large as 500 MPa for the same sample. Optical microscopy of microspecimens revealed several inhomogeneities near the surface by overlapping which may contribute to the large scattering in the residual stresses.

A wide range of industrial applications employs components, manufactured by full-forward extrusion. The process can either be performed at room temperature or at elevated temperatures [13]. Hot extrusion above the material's recrystallization temperature is often performed to prevent work hardening and decrease the

demanded forming forces. However, if the process is performed at room temperature (cold extrusion), the final products present some important advantages: lack of oxidation, better surface finish, maintenance of smaller tolerances and higher strength due to cold working [14]. In the case of cold extrusion, high forces and tribological loads characterize the process. Therefore, special attention should be paid to the material and to the coating of the working tools, especially of the forming die, to avoid fast wear. Secondly, in order to decrease the forming forces and the loads on the working tools, the friction conditions must be optimized. To reduce the high tribological loads in the forming region and surface expansion, an appropriate tribological system should be employed. In the cold extrusion of austenitic stainless steels, a two-layer lubricant system consisting of a conversion layer and a lubricant layer is commonly used [15]. Molybdenum disulfide (MoS_2) is a typical dry lubricant for these applications at room temperature. For the conversion layer, oxalate is a common choice for stainless steels, while phosphate is used for carbon steels.

Cold extrusion of metals generally leads to highly unfavorable residual stress states [16]. In the axial direction, the resulting first-order residual stresses are highly tensile on the component surface of the workpiece and compressive in the middle. This distribution is strongly undesired for components subject to cyclic loads. The tensile residual stresses on the surface facilitate the formation and propagation of cracks reducing the fatigue life of such components significantly [17]. The origin of the macroscopic residual stresses in cold massive forming processes is mainly caused by inhomogeneous (plastic) deformation inside the workpiece [18]. In particular, this phenomenon is due to the different material flow conditions that affect the surface and the center of the metal part during the forming process [19]. The material can flow purely axially in the center of the extruded part, while the surface is constrained in axial and radial direction by the shoulders of the forming die and undergoes shear forces coming from the friction.

2 Materials and Methods

The billets of 1.4404 were procured from the same batch of material. The specimens were then milled into cylinders with a diameter of 14.5 mm and a length of 50 mm. Then, the specimens were annealed in a vacuum oven at 1050 C° for 15 min. To achieve a better adhesion of coatings, the samples were shot peened. As the aim of the shot peening process was a more suitable surface state for coating, the parameters were not chosen in a way to produce a uniform compressive residual stress state. Afterward, a tribological coating system of two layers was applied on the surface of the samples to assure adequate coefficients of friction and resistance: a first conversion layer with oxalate and a second layer with the MoS_2-based lubricant ZWEZ-Lube MD 230. A mark was graved on each sample before the forming operation in order to allow the tracking of the measuring point on the extruded samples. Four specimens are being investigated in this study, which are numbered 1 to 4 and were prepared identically by annealing, shot peening, coating and cold extrusion.

The samples were then cold extruded to the final diameter of 10.78 mm. The parameters of the forming operation are displayed in Fig. 1. The initial diameter in the figure refers to the opening of the forming die.

The axial residual stresses of the billets were measured in the initial state to allow a comparison of the stress states before and after cold extrusion. The samples were measured following a central experiment design. The positions of the measurements on the samples were defined in relation to the mark as well as the center of the samples. The center of the rhomb-shaped measurement pattern was defined as position 0 mm (30 mm from the mark) at a relative angle of 0°. Along this axis, two additional measurement points were located at a distance of 14 mm (± 14 mm/0°). Along the circumferential direction, measurement points are located at a distance of 63.5° (0 mm/ ± 63.5°). The measurement points oriented between the cardinal directions are situated 10 mm and 45° from the center (± 10 mm/ ± 45°). This pattern is shown in Fig. 2 for both schematic representation as well as a picture of the samples before and after cold working. The order of measurements was randomized within those of a single sample. The position in the center was measured four times due to the relative importance of the results.

The residual stresses were determined by X-ray diffraction (XRD) according to DIN EN 15,305:2009–01 using the $\sin^2 \Psi$-method. Therefore, a diffractometer made by Stresstech, model XStress G3R in a modified Ψ-arrangement was used. The residual stresses were calculated from seven equidistant Ψ angles ranging from 0° to + 45° and from 0° to − 45°, respectively. Mn Kα radiation was used for the measurement of the residual stresses of the reflex (311) in the fcc austenitic lattice structure. A rectangular aperture with a length of 3 mm and a width of 1 mm was used to maximize the size of the irradiated area, while minimizing the effect of the samples' curvature, compared to a circular aperture. The longer side of the rectangle was aligned in the direction of the Ψ rotation. As the axial component of the residual stress state was measured, the long side of

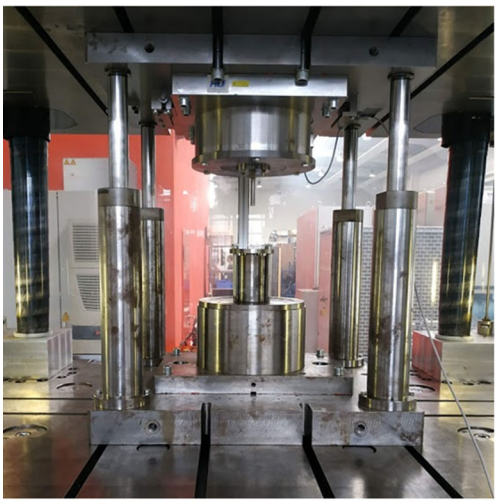

Forming parameters	
Forming speed	2.3 mm/s
Forming Die	
Material	Carbide G20
Coating	TiAlN
Opening angle	60°
Length calibration zone	2 mm
Initial diameter	14.7 mm
Final diameter	10.78 mm

Fig. 1 Extrusion process Synchropress SWP 2500, extrusion tools and forming parameters

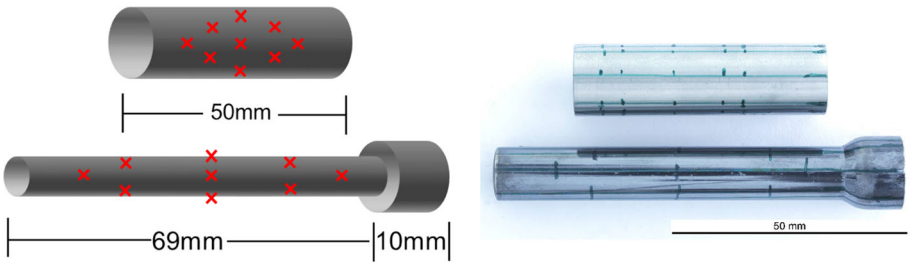

Fig. 2 Left: Schematic representation of the sample in the original state and after cold working with markers for the measurement points. Right: exemplary picture of the samples

the rectangle is oriented along the axial direction of the samples. The X-ray elastic constant used to calculate the residual stress values was ½S2 $\{311\} = 7.57 \times 10^{-6}$ mm^2/N for austenite [20]. Furthermore, sample 3 was measured with a Ψ oscillation of $\pm 6°$ to increase the statistical number of grains that satisfy the diffraction condition to satisfy the criterion for significant measurement results [5]. The peak fit was performed using the cross-correlation method.

After the extrusion process, the samples were measured again. The new measurement positions were chosen such that they correspond to the positions before cold extrusion. As the measured area of the sample was elongated from 40 to 69 mm, the new center of measurements was at 45 mm from the mark. Due to the position being measured from the center, the center retained the coordinates of 0 mm and 0°. For the other measurement points, the distances from the center were multiplied by a factor of 1.8 to describe the elongation and keep the measured positions identical. This resulted in distances of 18 mm and 25 mm. The new measurement positions are: 0 mm/0°; $\pm$ 18 mm/$\pm$45°; 0 mm/$\pm$63.5° and $\pm$25 mm/0° (see Fig. 2), but are normalized to the distance of the initial state samples (see Fig. 3). The order of measurements for individual samples was randomized after cold extrusion as well.

After measuring both the initial state as well as the cold extruded state, the samples 2 and 4 were stripped of the lubricant by chemical etching. First, they were submerged in 5% alkaline solution/base at 80 °C for 10 min. After rinsing with water, they were exposed to 10% sulfuric acid at room temperature for 3 min. After this procedure, they were measured again with the same parameters, including randomized order of measurements.

In addition, microspecimens were prepared to examine the materials' microstructure before and after cold deformation by optical microscopy.

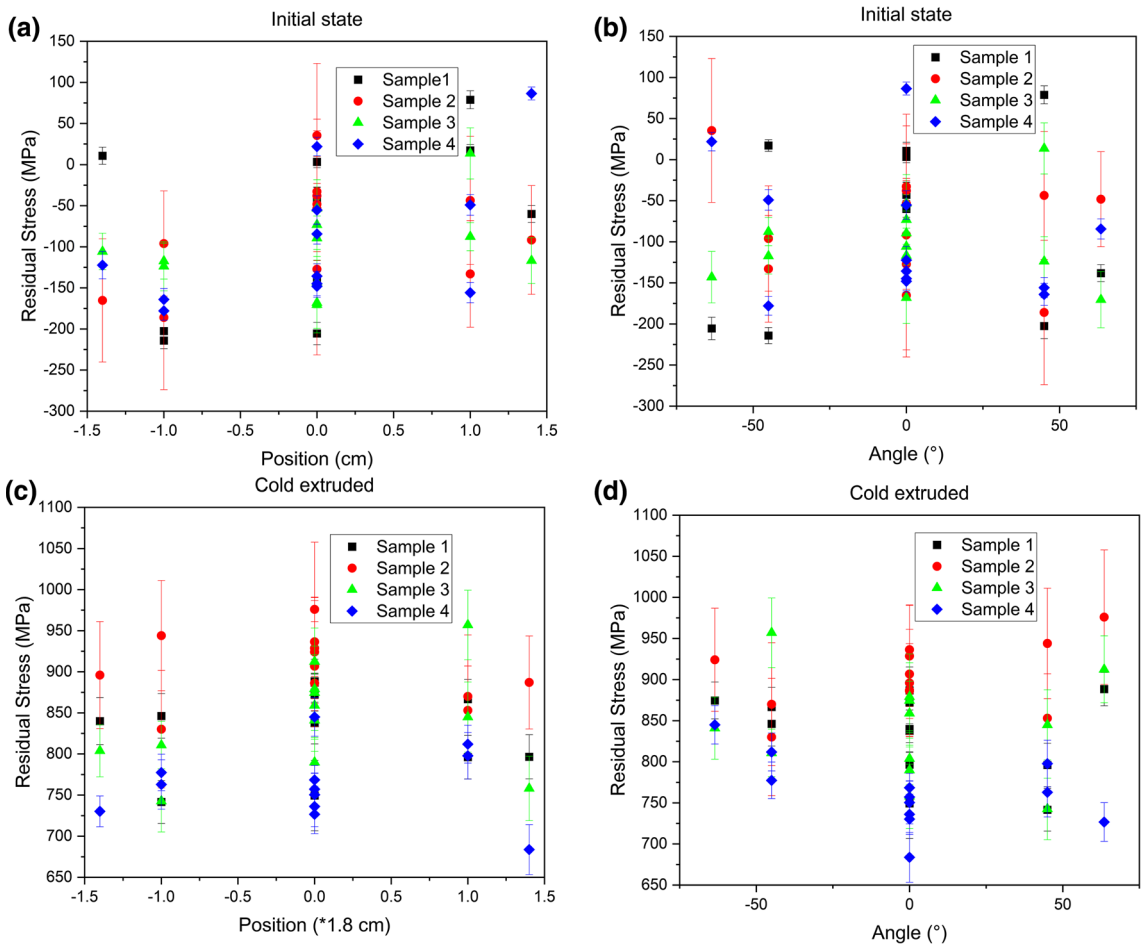

Fig. 3 Comparison of the axial residual stresses for samples 1 to 4. The results are plotted for: **a** the initial state as a function of the position **b** the initial state as a function of the angle **c** after cold extrusion as a function of the position **d** after cold extrusion as a function of the angle

3 Results and discussion

3.1 Analysis of residual stress

Figure 3 displays the results of the X-Ray measurements of the residual stresses in the four samples before and after the forming operation. The values are shown and compared for the single measured positions, according to the pattern described in Fig. 2. While the initial state shows residual stresses around 0 MPa in a range from − 300 MPa to 100 MPa, the cold extrusion causes residual stresses between 700 and 900 MPa. In the extruded state, the samples display a scattering between the different measured points of approximately 200 MPa. Interlaboratory tests, in which different flat samples with a defined stress state were measured as part of the research program SPP 2013, showed a scattering distance of ± 50 MPa. This is less than the results for the cylindrical samples in the initial state. With the samples differing to this degree in the initial state, the question arises, if a correlation between the residual stresses before and after extrusion exists. This was addressed by means of a statistical analysis.

To quantify the effect of the longitudinal position and the angle of the measurements, the measurement results were used to calculate a quadratic regression for all four samples as well as the individual samples in both the initial and the cold extruded state. The results are shown in Table 1. The modelling equation has the form:

Table 1 Coefficients for the quadratic regression fit for the initial, cold extruded, and cold extruded and etched state

State	Samples	a (MPa)	b (MPa/mm)	c (MPa/°)	d (MPa/mm^2)	e (MPa/°^{2})	f (MPa/mm°)
Initial	1–4	**− 77.2**	112	**35.5**	− 210	− 12.6	135
Initial	1	**− 28.80**	730	29.7	1330	− 133.8	250
Initial	2	**− 62.80**	370	− 20.9	− 8930	32.7	895
Initial	3	**− 96.00**	267	10	1240	− 33	537
Initial	4	**− 120.80**	765	− 42.90	4690	33.30	− 600
Cold extruded	1–4	**838.7**	− 153.7	9.85	− 2168	15.38	− 88
Cold extruded	1	**836.6**	24	− 27.5	− 3700	26.2	170
Cold extruded	2	**914.6**	− 113	30.1	− 4630	12.1	− 653
Cold extruded	3	**850.60**	325	− 14.00	− 6480	31.00	− 219
Cold extruded	4	**753**	7	− 34.6	− 2550	53.4	2
Cold extruded and etched	2	**913.58**	0.7	**35.24**	**− 4980**	1.9	**− 580**
Cold extruded and etched	4	**735.1**	− 131	**− 37**	− 2880	**50.6**	− 134

Entries that have a P value of less than 5% are marked in bold (see Table 2). In the cases, where all samples were viewed in their entirety all data points were treated equally, independent of on which sample they were measured

$$\sigma = a + b \cdot L + c \cdot A + d \cdot L^2 + e \cdot A^2 + f \cdot LA \tag{1}$$

where σ is the residual stress, L the length from the middle of the sample (times 1.8 for the cold extruded case) and A the angle. The lowercase letters a to f are fitting coefficients that indicate the interaction between the variation of the measurement position in the length and angle and the measured residual stress. The results of the fitting coefficients are shown in Table 1. The Table also contains the coefficients for the samples 2 and 4 after etching. These samples will be considered in more detail in the following parts of the paper to investigate the influence of the coating layer on the residual stress measurements. It can be seen that the values of the fitting coefficients for different samples in the same state scatter to a large degree. This is especially noticeable for the coefficients regarding the factors connected to the position and angle, while the coefficient which only tracks the different samples varies less. The large scatter of the variables connected to linear and quadratic correlation imply that there is no common correlation between where the measurement is performed and the measured residual stresses.

A quadratic regression was used to check for possible linear and quadratic relations between longitudinal position and angle and the measured residual stress. The employment of a higher order regression would not have been appropriate due to the limited number of data points. With the assumption of symmetry between positive and negative angles, the measurements were performed at only 3 independent angles. Thus, there are only three data points available for calculating the variables for each direction (position and angle). This means that only three independent variables can be calculated, which in this case are the constant offset, the linear dependency and the quadratic dependency. To check for a correlation between position and angle and the result of the residual stress measurements of a higher order, additional measurement points would have to be chosen.

To define the quality of the regressions, the P value is calculated for the constants of the modelling equation (see Table 2). The null hypothesis was rejected for P values smaller than 0.05. The P values for the fitting coefficients are displayed in Table 2.

It can be seen that the constant a, whose effect is not dependent on the length (L) or angle (A), is the only factor which satisfies the rejection criteria of the null hypothesis in the vast majority of cases. The coefficient for the linear dependence on the angle for all samples in the initial state and the coefficient for the quadratic dependence on the angle of the second sample in the original state and all samples in the cold extruded state allow the rejection of the null hypothesis as well, but in the context of the majority of P values accepting the null hypothesis, it can be assumed that this is the result of statistical scattering. The cold extruded and etched samples show a higher frequency of rejecting the null hypothesis. This supports the assumption made from the scatter of the coefficients (see Table 1) that there is no evidence of systematic correlation between measurement position and angle and the measured residual stress. The only variable that has a consistent correlating effect is which sample of the set was measured (coefficient a).

For further analysis of the residual stress data, the arithmetic mean, standard deviation and confidence interval (95%) are shown in Table 3. For the initial state, the confidence intervals exhibit a large overlap with all the arithmetic means being inside the other samples' confidence intervals as well (with the exception of

Table 2 *P* Values of the constants from Table 1

State	Samples	*a* (MPa)	*b* (MPa/mm)	*c* (MPa/°)	*d* (MPa/mm^2)	*e* (MPa/°^{2})	*f* (MPa/mm°)
Initial	1–4	**0**	0.383	**0.008**	0.884	0.38	0.456
Initial	1	0.547	0.158	0.535	0.858	0.11	0.791
Initial	2	**0.031**	0.148	0.384	**0.045**	0.389	0.092
Initial	3	**0.016**	0.391	0.742	0.795	0.497	0.389
Initial	4	**0.019**	0.091	0.301	0.464	0.599	0.457
Cold extruded	1–4	**0**	0.056	0.215	**0.017**	0.086	0.432
Cold extruded	1	**0**	0.938	0.39	0.461	0.597	0.785
Cold extruded	2	**0**	0.506	0.108	0.116	0.648	0.086
Cold extruded	3	**0**	0.375	0.693	0.272	0.583	0.757
Cold extruded	4	**0**	0.973	0.117	0.426	0.124	0.995
Cold extruded and etched	2	**0**	0.995	**0.002**	**0.004**	0.904	**0.008**
Cold extruded and etched	4	**0**	0.326	**0.011**	0.179	**0.024**	0.611

P values lower than 0.05 mean that the null hypothesis of the connected variable not having an influence can be safely rejected. Accepted *P* values are marked in bold. In the cases, where all samples were viewed in their entirety all data points were treated equally, independent of on which sample they were measured

Table 3 Arithmetic mean, standard deviation and confidence interval of the residual stress for the samples 1 to 4 in the initial, cold extruded, and initial and cold extruded state

State	Sample	Arithmetic mean (MPa)	Standard deviation (MPa)	Confidence interval (95%)
Initial	1	− 69.1	98.1	(− 131.4; − 6,8)
Initial	2	− 81.7	63.4	(− 122.0; − 41.4)
Initial	3	− 102.9	51.0	(− 135.3; − 70.5)
Initial	4	− 94.1	81.7	(− 146.0; − 42.2)
Cold extruded	1	833.0	51.0	(800.6; 865.5)
Cold extruded	2	903.2	41.3	(877.0; 929.4)
Cold extruded	3	839.4	62.4	(799.7; 879.1)
Cold extruded	4	762.3	42.8	(735.1; 789.5)
Cold extruded and etched	2	897.6	41.0	(880.3; 914.9)
Cold extruded and etched	4	742.5	46.8	(722.7;762.2)

sample 1 being outside the confidence interval of sample 3). Additionally, a larger standard deviation can be observed from the results of samples 1 and 4. The standard deviation of sample 3 is smaller than for sample 2. This could be a beneficial effect of the increased number of diffraction planes by the Ψ-oscillation. After the cold extrusion process, the arithmetic means diverge to larger degrees and the confidence intervals only overlap between samples 1 and 3. This shows that the residual stress states of the samples differ after cold extrusion. The etching of the cold extruded sample 2 leads to a slight decrease of the residual stress, while not influencing the standard deviation. Sample 4, however, exhibits a small drop in residual stress and a rise in the standard deviation. The data spread can be assigned to normal microstructure effects during the deformation process, if differently oriented grains are deformed. This leads to different results in the measurements as well.

For the initial state, the applied shot peening procedure is a process of multiple singular collisions and can lead to local deviations from a uniform stress state. For the cold extrusion process, local deviations of the residual stress state can be caused by changes in the friction conditions due changes in the thickness of the lubrication layer. The differences between the different samples both in the initial state and after cold extrusion are in the normal ranges for the repeatability of both processes, although it is worth mentioning that the inter-sample differences decreased after the deformation process.

3.2 Effect on the FHWM

Of similar interest to the residual stress is the full width at half maximum (FWHM) of the diffraction reflexes. A higher value denotes a larger density of defects [21]. In the initial state, the samples 2 and 3 exhibit lower FWHMs between 1.5° and 2.5° than the samples 1 and 4 between 3.0° and 4.0° (see Fig. 4). Similar to the results for the residual stress, there is no correlation between length and angle and the FWHM value evident.

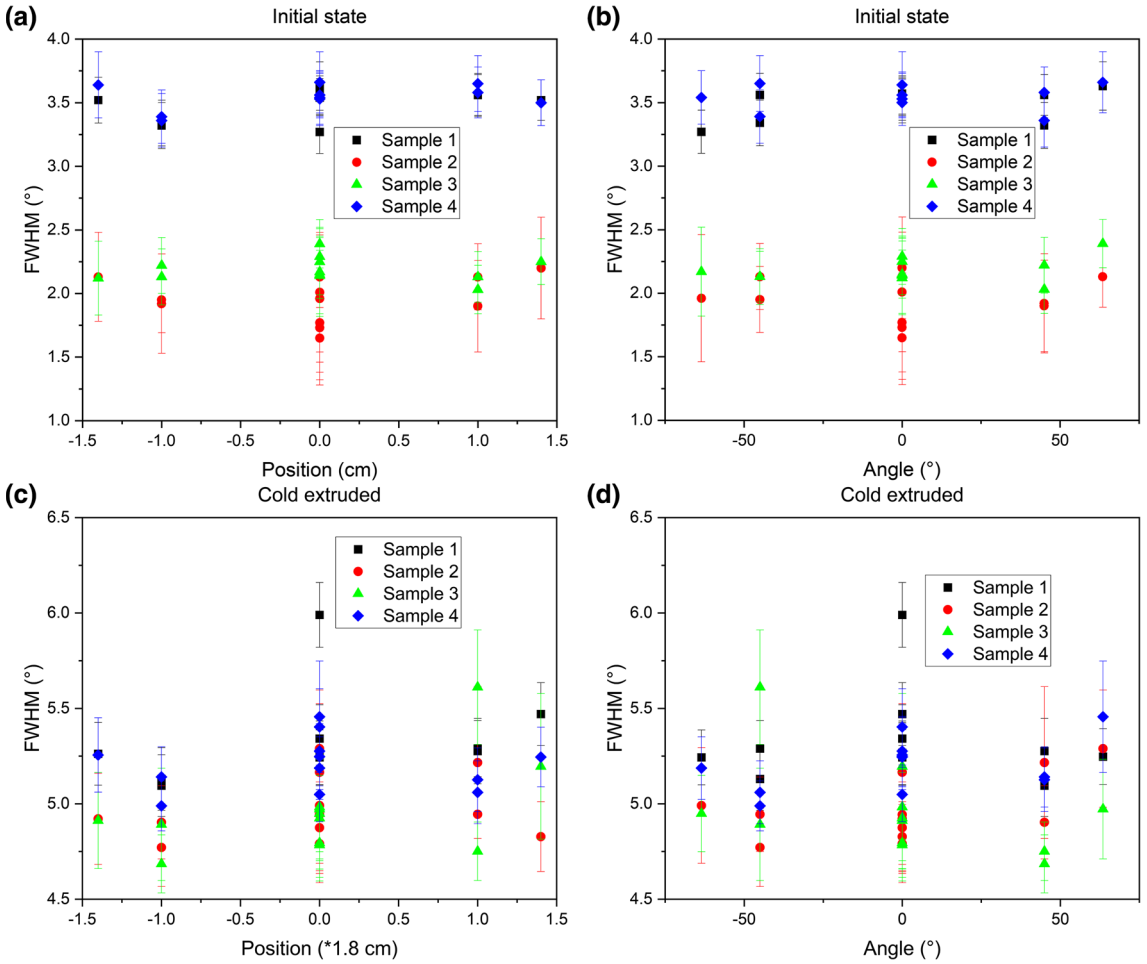

Fig. 4 Comparison of the full width at half maximum (FWHM) for samples 1 to 4. The results are plotted for: **a** the initial state as a function of the position **b** the initial state as a function of the angle **c** after cold extrusion as a function of the position **d** after cold extrusion as a function of the angle

After cold extrusion, the difference in FWHM values between samples 1 and 4 and samples 2 and 3 disappears. All samples exhibit values between 4.5° and 5.5°. This would suggest that the samples exhibit more defects after the cold extrusion process (compare Fig. 6).

To understand the change in FWHM, exemplary signal peaks for measurements at position 0 cm/0° at a Ψ-angle of 0° are compared for the initial state as well as the cold extruded state (see Fig. 5). As expected from the FWHM values, the signal peaks are broader after extrusion than in the initial state. Moreover, they show significantly lower scattering. The maximum of the peaks in the cold extruded state is much lower than for the samples in the initial state. All cold-extruded samples exhibit similar signal-to-noise ratios, which are lower than those of the initial state samples. However, the peaks of the samples with lower FHWM values (2 and 3) are much narrower and have higher maximums. Additionally, the maximum is shifted to lower angles for the narrower peaks.

In order to identify the causes of the differences in the signal peaks (see Fig. 5), the microstructures of the samples 1 and 3 are analyzed before and after cold extrusion by optical microscopy (see Fig. 6). It is evident that sample 1 shows an abundance of slip line defects in the surface near area. This is not the case for sample 3, where no slip lines are visible. Since all samples had been annealed after the machining, there are not many possibilities, how only some of them obtained those defects. It is likely that the defect structures (slip bands) are caused by the shot peening process preceding the coating of the sample. It lead to the formation of slip lines in sample 1, while those are absent in sample 3. These slip lines near the surface are in good agreement with the peak broadening. Interestingly, these microstructural differences in the initial state did not have a significant effect the formation of residual stresses after extrusion. The same can be said for the FWHMs. The

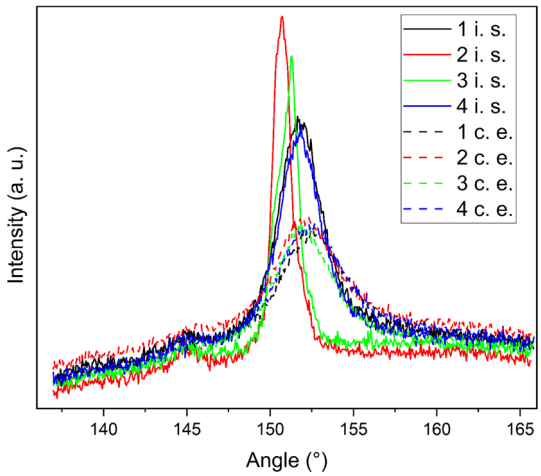

Fig. 5 Comparison of exemplary signal peaks for measurements at position 0 cm/0° and a Ψ-angle of 0° for samples 1 to 4 in the initial (i.s.) and cold extruded (c.e.) state

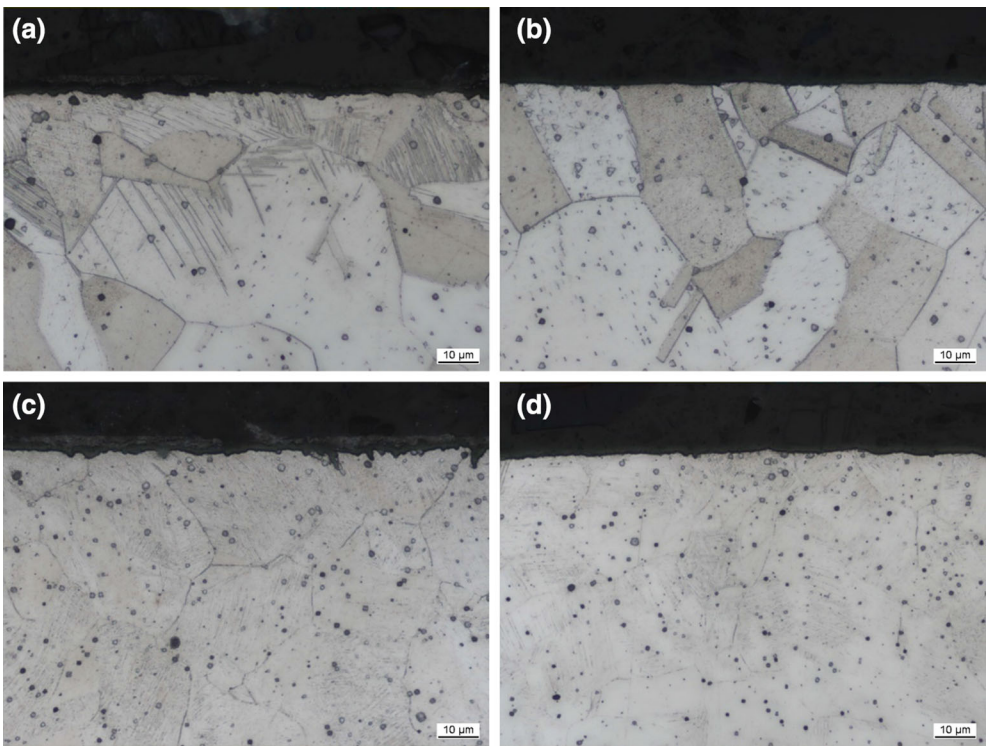

Fig. 6 Comparison of the microstructure of the samples 1 and 3 in the initial and cold extruded state. **a** Sample 1 in the initial state **b** sample 3 in the initial state **c** sample 1 in the cold extruded state **d** sample 3 in the cold extruded state

results for the cold extruded state are the identical (see Fig. 4). This is in accordance with the micrographs, where no difference between sample 1 and sample 3 can be detected (Fig. 6c and d).

3.3 Effect of the coating

Samples of stainless steel 1.4404 require appropriate tribological systems to be extruded at room temperature, typically a two-layer coating as described in this paper. An interesting question is whether and how this coating affects the measurements though X-ray diffraction of the residual stresses. If the effect of the coating on the

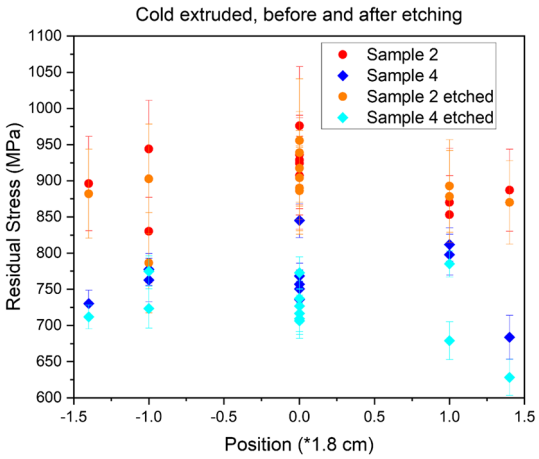

Fig. 7 Axial residual stresses as a function of the position along the samples 2 and 4 after cold extrusion and after etching following the cold extrusion

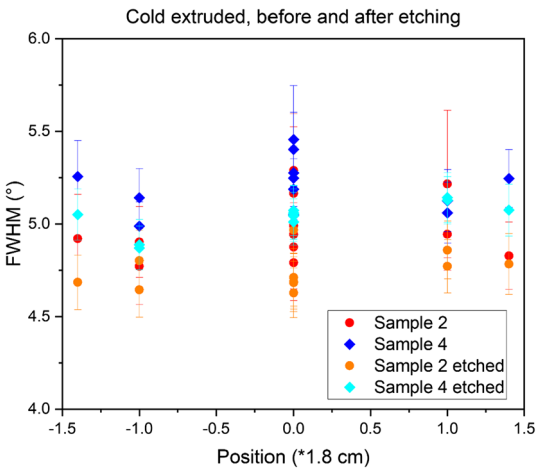

Fig. 8 Full width at half maximum (FWHM) as a function of the position along the samples 2 and 4 after cold extrusion and after etching following the cold extrusion

measurements is significant, possible defects in the coating conditions should be considered in the study and could explain small scattering in the measuring points. Therefore, an etching process was performed to analyze the effect of the oxalate and MoS_2 layers on the X-ray diffraction measurements, as described in the previous chapter. The results of the stress measurements before and after etching are shown in Fig. 7. There are no observable effects on the residual stresses for sample 2, while the residual stress for sample 4 is marginally lower after the etching process than before it. As shown in Table 1, there is no consistent correlation between angle and length and the residual stress state.

The FWHM results (Fig. 8) show that for both samples the etching process resulted in lower FWHM values, which points toward smaller defect densities. Without the oxalate and MoS_2 layers, the X-rays penetrate into deeper regions, which means that parts of the sample further away from the surface are measured. As the defect density is highest at the surface after the cold deformation, the FWHM is smaller, if more volume of the material below the surface is measured. The average information depth of Mn K_α-radiation in austenitic steels is 7.2 μm [1]. The absorption of the thin (1–3 μm) MoS_2 layer can be estimated to be less due to the lower density and two thirds of the atoms having a lower atomic number than Fe. The exact increase in penetration depth into the austenitic steel due to the removal of the MoS_2 layer cannot be measured by the method used to determine the residual stresses. To assess the residual stress measurement strategy, residual stresses were measured with MoS_2 and after chemical removal of the layer. Both the peak quality and the calculated residual were not affected by the thin MoS_2 layer.

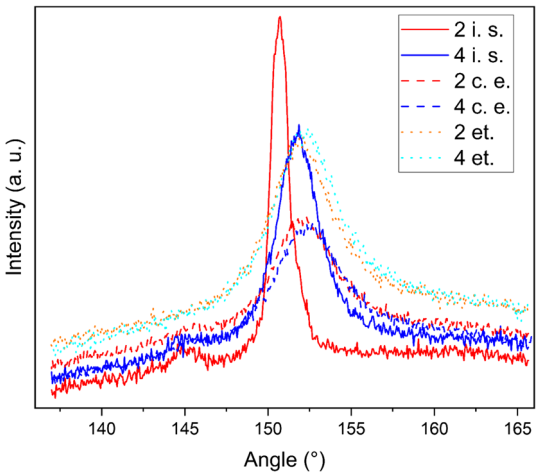

Fig. 9 Comparison of exemplary signal peaks for measurements at position 0 cm/0° and a Ψ-angle of 0° for samples 2 and 4 in the initial (i. s.). cold extruded (c.e.) and cold extruded and etched (et.) state

Similar to Fig. 5, exemplary signal peaks for measurements at position 0 cm/0° at a Ψ-angle are shown in Fig. 9 with the inclusion of measurements in the cold extruded and etched state. The background level of the etched samples is elevated in comparison to the two other states. While the same is true for the height of the peaks, the peaks shape is not different compared to the measurements before the removal of the coating. The higher intensity is caused by absence of the coating, which increases the penetration depth of the x-rays into the sample.

4 Conclusion

In the present paper, the uniformity of the stress state in cold extruded parts of stainless steel 1.4404 was statistically examined, as well as the causes for scattering in the measured residual stresses. It was observed that, while some scattering (50 MPa) can be attributed to the uncertainty of the measurement method, the initial state of the samples after coating with lubricants, but before cold extrusion, varies regarding the residual stresses as well as the FWHM and the microstructure.

By measurement of the cold extruded samples, it was proven that the residual stress state created by the cold extrusion method is robust in relation to the residual stress state and the presence of slip lines in the material before the deformation. The residual stress states and microstructures are not influenced by small deviations in microstructure present in a previous material state. The scattering after deformation is mainly caused by local variations in grain orientation and differences in the thickness of the lubrication layer and the resulting changes in the shear processes. While local variations of the residual stress state still exist, they are smaller than for the initial state.

An effect of the variation of the length and the angle of the measurement position on the measured residual stress and FWHM on samples produced by cold extrusion could not be proven. The macroscopic stress can be represented by only one measurement on a homogenous cold extruded specimen, where a higher measurement uncertainty must be considered in comparison to the error from the $\sin^2 \Psi$ plot of one single measurement. The uncertainty of the residual stress after 12 measurements in the cold extruded state is between 50 and 80 MPa. The residual stress state is more homogeneous after cold extrusion than in the initial state. The scatter distance of 200 MPa fit with results from the literature, which measured the residual stresses along the axial position.

Removal of the oxalate and MoS_2 layer by etching lead to a small decrease in both residual stress and FWHM, but did not change the result in a way that would prevent the method from being used for future measurements. The effect of the etching on the intensity and uncertainty of singular measurements was negligible and the shape of the peaks did not diverge much from the cold extruded state despite exhibiting lower intensities. The individual results after cold extrusion and after etching being similar reinforces the conclusion

that the scattering of the results is not caused by the measurement process, but differences in the localized residual stress state.

Funding Open Access funding enabled and organized by Projekt DEAL. This work was supported by the Deutsche Forschungsgemeinschaft (DFG, German Research Foundation) in the framework of the priority program SPP 2013 ("Residual Stresses") by a Grant OE 558/16-1 and GR 1818/63-1.

Data availability All data is archived and available upon request in accordance with the requirements of the priority program.

Code availability Not applicable.

Declarations

Conflict of interest On behalf of all authors, the corresponding author states that there is no conflict of interest.

Open Access This article is licensed under a Creative Commons Attribution 4.0 International License, which permits use, sharing, adaptation, distribution and reproduction in any medium or format, as long as you give appropriate credit to the original author(s) and the source, provide a link to the Creative Commons licence, and indicate if changes were made. The images or other third party material in this article are included in the article's Creative Commons licence, unless indicated otherwise in a credit line to the material. If material is not included in the article's Creative Commons licence and your intended use is not permitted by statutory regulation or exceeds the permitted use, you will need to obtain permission directly from the copyright holder. To view a copy of this licence, visit http://creativecommons.org/licenses/by/4.0/.

References

1. Withers, P.J.: Residual stress and its role in failure. Rep. Prog. Phys. **70**(12), 2211 (2007)
2. Macherauch, E.: Neuere Untersuchungen zur Ausbildung und Auswirkung von Eigenspannungen in metallischen Werkstoffen. Mat.-wiss. u. Werkstofftech. https://doi.org/10.1002/mawe.19790100309
3. Reiss, A., Engel, U., Merklein, M.: Investigation on the influence of manufacturing parameters on the Fatigue strength of components. KEM (2011)
4. Withers, P.J., Bhadeshia, H.: Residual stress. Part 2-Nature and origins. Mater. Sci. Technol. (2000). https://doi.org/10.1179/026708301101510087
5. Hoche, H., Balser, A., Oechsner, M. et al.: Verbesserung des Eigenspannungszustands beim Kaltfließpressen durch den aktiven Einsatz eines gesteuerten Gegenstempels: Enhancement of the residual stresses of cold full-forward extruded parts by application of an active counter punch. Materialwiss. Werkstofftech. https://doi.org/10.1002/mawe.201900050
6. Lee, H.H., Gangwar, K.D., Park, K.-T., et al.: Neutron diffraction and finite element analysis of the residual stress distribution of copper processed by equal-channel angular pressing. Mater. Sci. Eng. (1984). https://doi.org/10.1016/j.msea.2016.11.094
7. Landkammer, P., Jobst, A., Kiener, C., et al.: Investigations on residual stress generation in full-forward-extrusion. Prod. Eng. Res. Devel. (2019). https://doi.org/10.1007/s11740-019-00892-5
8. Hoche, H., Jaeger, F., Franceschi, A. et al.: Formation of residual stresses in austenitic stainless steels by infeed and recess rotary swaging. In: To be published in Proceedings 13th International Conference on the Technology of Plasticity (ICTP 2021). https://doi.org/10.31224/osf.io/6uks7
9. Gerin, B., Pessard, E., Morel, F., et al.: Beneficial effect of prestrain due to cold extrusion on the multiaxial fatigue strength of a 27MnCr5 steel. Int. J. Fatigue (2016). https://doi.org/10.1016/j.ijfatigue.2016.07.012
10. Wolfstieg, U., Macherauch, E.: Ursachen und Bewertung von Eigenspannungen. Chemie Ing. Technol. (2000). https://doi.org/10.1002/cite.330451103
11. Franceschi, A., Jaeger, F., Hoche, H., et al.: Calibration of the residual stresses with an active die during the ejection phase of cold extrusion. Int. J. Mater. Form (2020). https://doi.org/10.1007/s12289-020-01572-x
12. Simon, N., Erdle, H., Walzer, S., et al.: Phase-specific residual stresses induced by deep drawing of lean duplex steel: measurement vs. simulation. Prod. Eng. Res. Devel. (2019). https://doi.org/10.1007/s11740-019-00877-4
13. Doege, E., Behrens, B.-A.: Handbuch Umformtechnik. Springer, Berlin (2016)
14. Tiernan, P., Hillery, M.T., Draganescu, B., et al.: Modelling of cold extrusion with experimental verification. J. Mater. Process. Technol. **168**(2), 360–366 (2005)
15. Bay, N.: The state of the art in cold forging lubrication. J. Mater. Process. Technol. (2020). https://doi.org/10.1016/0924-0136(94)90100-7
16. Lange, K., Tekkaya, A.E.: Ermittlung von Eigenspannungen in der Kaltmassivumformung. Springer, Berlin (1986)
17. Withers, P.J.: Residual stress and its role in failure. Rep. Prog. Phys. (2012). https://doi.org/10.1088/0034-4885/70/12/R04
18. Withers, P.J., Bhadeshia, H.: Residual stress. Part 1-Measurement techniques. Mater. Sci. Technol. (2010). https://doi.org/10.1179/026708301101509980
19. Zhang, H., Zhao, X., Deng, X., et al.: Investigation of material flow during friction extrusion process. Int. J. Mech. Sci. (2014). https://doi.org/10.1016/j.ijmecsci.2014.05.011
20. Eigenmann, B., Macherauch, E.: Röntgenographische Untersuchung von Spannungszuständen in Werkstoffen. Teil III.. Fortsetzung von Matwiss. und Werkstofftechn. Heft **27**(9), 426–437 (1996)

21. Spieß, L., Teichert, G., Schwarzer, R., Behnken, H., Genzel, C.: Moderne Röntgenbeugung: Röntgendiffraktometrie für Materialwissenschaftler, Physiker und Chemiker, 2nd edn. Springer, Wiesbaden (2009)
22. DIN EN 15305:2009-01: Zerstörungsfreie Prüfung_- Röntgendiffraktometrisches Prüfverfahren zur Ermittlung der Eigenspannungen; Deutsche Fassung EN_15305:2008. Berlin: Beuth Verlag GmbH

Publisher's Note Springer Nature remains neutral with regard to jurisdictional claims in published maps and institutional affiliations.